Jpn. J. Appl. Phys. Vol. 41 (2002) pp. 2090–2093
Part 1, No. 4A, April 2002

Electronic Structure of 4*d* Transition Metal Compound ZrF_4 by Resonant Photoemission Spectroscopy

Tohru HIGUCHI*, Takeyo TSUKAMOTO, Shu YAMAGUCHI[1], Yasuhisa TEZUKA[1] and Shik SHIN[2,3]

Department of Applied Physics, Science University of Tokyo, Tokyo 162-8601, Japan
[1]*Hirosaki University, Hirosaki 036-8561, Japan*
[2]*Institute for Solid State Physics, University of Tokyo, Chiba 279-8581, Japan*
[3]*RIKEN, Hyogo 679-5143, Japan*

(Received August 10, 2001; accepted for publication January 11, 2002)

The electronic structure of 4*d* transition metal compound ZrF_4 has been studied by resonant photoemission spectroscopy. A satellite structure is found at the higher binding energy side of the main peak of the valence band with an energy separation of about 12.6 eV. The intensity of the valence band as well as its satellite structure is resonantly enhanced at the excitation energy threshold of Zr 4*p*. The existence of the satellite can be explained by the strong hybridization effect between Zr 4*d* and F 2*p* states in the valence band. [DOI: 10.1143/JJAP.41.2090]

KEYWORDS: ZrF_4, electronic structure, resonant photoemission spectroscopy (RPES), satellite, hybridization

1. Introduction

Light 4*d* transition metals such as Zr or Ru show interesting electrical, structural, and magnetic properties. Superconducting materials have also been observed in layered nitride β-ZrNCl[1,2] and Sr_2RuO_4.[3] Furthermore, zirconium compounds are a very important ceramic material and have many applications such as oxygen sensor and artificial diamond. In spite of these interesting characteristics, the numbers of both theoretical and experimental studies on $4d^0$ transition metal compounds are few.[4–7] In terms of the electronic structure, it is well known that the 4*d* orbital is more widely extended than the 3*d* orbital and therefore the 4*d* electron correlation is expected to be weaker than the 3*d* electron correlation.

Many photoemission studies on 3*d* transition metals and their compounds have been reported. In heavy transition-metal oxides including Cu and Ni, it is known that the states arising from the $d^{n+1}\underline{L}$ configuration are mixed with those from the d^n configuration in the ground state, where *n* is the nominal number of 3*d* electrons and $\underline{L}$ represents the hole state in the O 2*p* states.[8] Such a charge-transfer (CT) material is also found in several light transition metal compounds.[9–16] In ScF_3, CT satellite structures are found with the energy separation of about 13 eV from main peaks in the valence band and various core energy regions.[13,14] However, the energy separation is too large compared to the magnitude of the CT energy of about 7–8 eV. Such a situation is also found in nominal $3d^0$ electron systems TiO_2 and V_2O_5. Okada and Kotani have calculated the CT satellite considering the many body configuration interactions.[10] They have indicated that large energy separation is mainly due to the large hybridization effect between the metal 3*d* orbital and the ligand 2*p* orbital rather than the CT energy.

In this study, we have examined the electronic structure of ZrF_4 by resonant photoemission spectroscopy (RPES). In $3d^0$ compounds such as Sc and Ti, the strong resonant enhancement has been found in fluoride rather than their oxides and extensively been discussed for the satellite structures.[13–17] Such a phenomenon can be expected in the $4d^0$ compound ZrF_4.

2. Experimental

The thin film of ZrF_4 was evaporated on a gold single-crystal substrate from the tungsten basket. In order to prevent the charging-up effect of the sample, the thickness of the sample was about 50–100 Å. The sample thickness was controlled by a quartz-crystal monitor. RPES spectra were measured at BL2 of SOR-RING at Synchrotron Radiation Laboratory, Institute for Solid State Physics, University of Tokyo. The synchrotron radiation was monochromatized using a grazing incidence spherical grating monochromator. The kinetic energy of the photoelectron was measured by a double-cylindrical-mirror analyzer. The overall energy resolution of the experimental system was about 0.3 eV. The measurement was carried out at room temperature. The position of the Fermi level was determined by measuring the Fermi edge of the Au film.

3. Results and Discussion

Figure 1(a) shows the total yield (TY) spectrum of ZrF_4, corresponding to the absorption spectrum from Zr 4*p* core-level to Zr 4*d* conduction bands. The vertical bars, which are numbered *1* to *12*, indicate the selected photon energies for the RPES measurements. The TY spectrum has a broad maximum at about 40 eV. This TY spectrum is very similar to 3*p* TY spectra of ScF_3 and TiF_3.[8,13,14] It is clear that the pre-edge structure at 34 eV is a multiplet structure formed by the strong 4*p*–4*d* interaction. The width of the main peak in ZrF_4 is due to the short lifetime of the super-Coster-Kronig decay process. The line shape might also be involved in the existence of the $4d^1\underline{L}$ states in ZrF_4, as will be discussed later.

Figure 1(b) shows the RPES spectra in the valence band region of ZrF_4 measured at various photon energies indicated in Fig. 1(a). The valence band is found around the binding energy of 10 eV, although the band gap of ZrF_4 has not been determined because there are neither absorption nor reflectance spectra of ZrF_4. The valence band spectra have two features, A and B, at 10.6 and 12.6 eV, respectively. The intensities of these features increase with increasing the excitation energy. In particular, the feature B in the valence band is enhanced at the excitation energy of

*E-mail address: higuchi@rs.kagu.sut.ac.jp

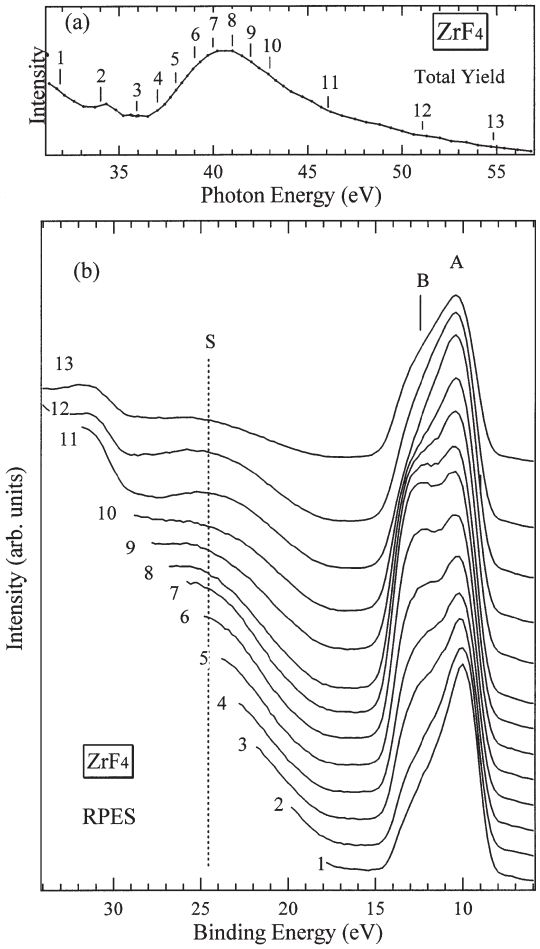

Fig. 1. (a) Total yield (TY) spectrum of ZrF_4 corresponding to the Zr 4*p* absorption spectrum. The numbers indicate the photon energies, where the RPES spectra have been measured. (b) Photoemission spectra in the valence band region excited at various photon energies indicated in (a).

40 eV. However, their intensities decrease at the excitation energy below 40 eV. On the other hand, the structure at around 32 eV, which is found in the photoemission spectra excited above $h\nu = 50$ eV, is the F 2*s* core line. A prominent feature signal S is observed at around 24.8 eV, indicating the existence of a satellite or Auger feature. The origin of signal S will be discussed later.

Figure 2 shows the constant initial state (CIS) spectra of ZrF_4 for features A, B, and S of Fig. 1. As reference, the TY spectrum of Fig. 1 is also shown. Three CIS spectra are measured at features A, B, and S. The location of the excitation threshold of the Zr 4*p* electron is indicated by the arrow. The threshold energy is estimated from the binding energy of the Zr 4*p* core level. These CIS spectra are governed by the excitation energy dependence of the ionization cross section. Both the valence band and signal S are resonantly enhanced above the 4*p* excitation threshold of the Zr^{4+} ion. This is a resonance in which pertinent holes in the final state are localized on the anion.

Figure 3 shows the comparison of (a) on- and (b) off-resonance spectra measured at $h\nu = 40$ and 36 eV, respectively. Both features A and B are resonantly enhanced by the Zr $4p \rightarrow 4d$ excitation in the on-resonance spectrum, although the resonance effect of feature A is very weak in comparison with that of feature B. The difference spectrum

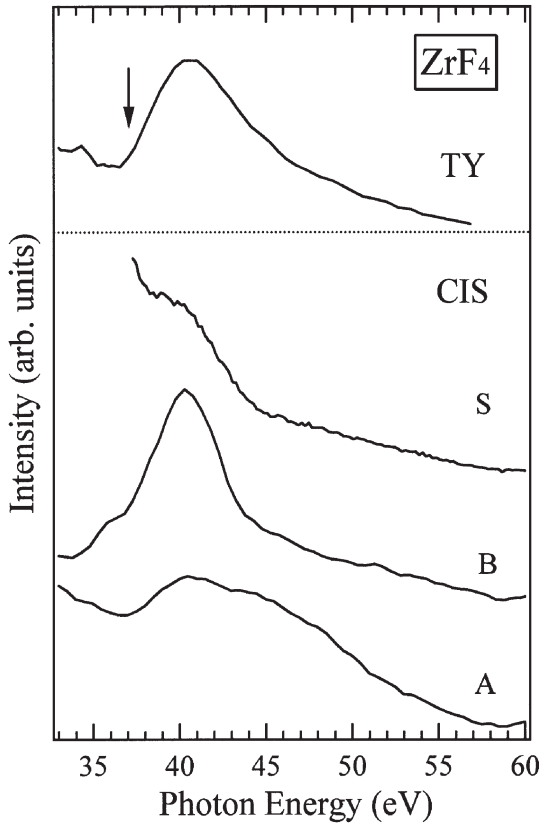

Fig. 2. Constant-initial-state (CIS) spectra of ZrF_4 for features A, B and S of Fig. 1.

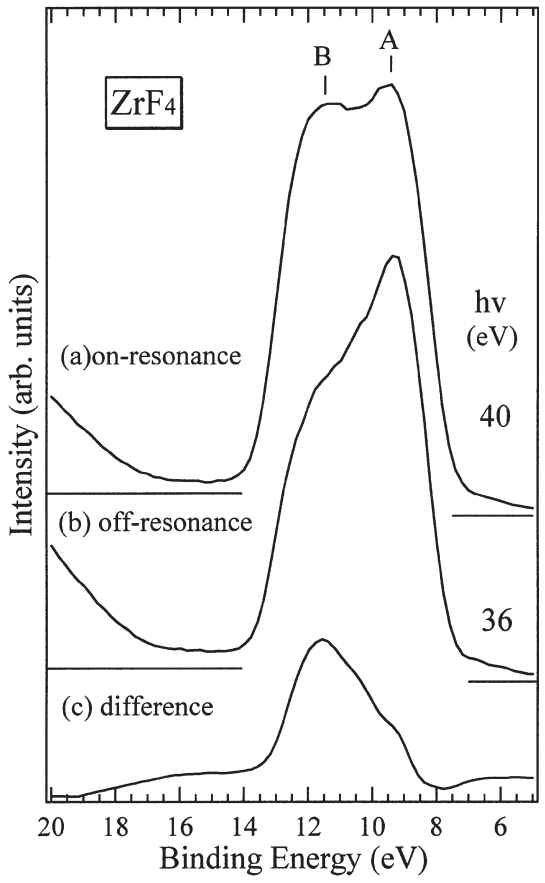

Fig. 3. (a) On-resonance and (b) off-resonance spectra measured at $h\nu = 40$ eV and 36 eV, respectively. (c) Difference spectrum from on-resonance to off-resonance spectra.

from the on-resonance to off-resonance spectra is shown in Fig. 3(c). The difference spectrum, which reflects the Zr 4*d* components in the valence band, has strong distribution on the feature B side. The Zr 4*d* contribution is more significant in the higher binding energy (feature B), where the O 2*p* states have a larger admixture of Zr 4*d* states. This shows that the indispensable magnitudes mix with the valence states. In other words, the valence states originating from the O 2*p* states are hybridized with the Zr 4*d* states. Therefore, we can estimate that the features arising from the bonding states occur at higher binding energy (feature B) and those from the nonbonding states at lower binding energy (feature A). In ZrO_2, it was reported that the Zr contribution is more significant in the higher binding energy region of the valence band, where the bonding O 2*p* states are expected to have a larger admixture of Zr 4*d* states. The covalent interaction between the Zr 4*d* and O 2*p* states is estimated to be about 24% in the bonding of ZrO_2. In ZrF_4, the covalent interaction is estimated to be about 30%.

Here, we discuss the origin of signal S observed in Fig. 1(b). The energy separation between the bonding peak of the valence band and signal S is ~12.6 eV. In terms of the 3*d* transition metal compounds, the energy separation is nominally determined by the CT energy Δ from ligand 2*p* to metal 3*d* orbitals. However, the observed separation is too large compared to the magnitude of Δ, which is about 7–8 eV. Furthermore, the CIS spectrum of signal S is resonantly enhanced at the same excitation energy as the bonding band. Therefore, the existence of signal S must be explained by the configuration interaction, where the $4d^1\underline{L}$ states for signal S are mixed with the $4d^0$ state for the valence band in the initial state due to the F 2*p*-Zr 4*d* hybridization. In the final states of the photoemission process, the valence band and the signal S structures are created from the $4d^0\underline{L}$ and $4d^1\underline{L}^2$ states. Thus, the large hybridization effect between Zr 4*d* and F 2*p* states is mainly reflected in the high splitting energy $\sqrt{\Delta^2 + 4V_{\mathrm{eff}}^2}$ ($\approx 2V_{\mathrm{eff}}$). Such a situation has been reported in ScF_3.[13,14]

Finally, we can understand the resonance enhancements of the valence band and signal S, assuming that the $d^1\underline{L}$ states are mixed with the d^0 state in the ground state. The excitation of the d^0 state leads to the $d^0\underline{L}$ state as

$$4d^0 + h\nu \rightarrow 4d^0\underline{L} + e. \quad \text{(a)}$$

Both $4d^0\underline{L}$ and $4d^1\underline{L}^2$ states are created through the direct excitation of the $d^1\underline{L}$ state as

$$4d^1\underline{L} + h\nu \rightarrow 4d^0\underline{L} + e, \quad \text{(b)}$$

$$\rightarrow 4d^1\underline{L}^2 + e. \quad \text{(c)}$$

In the resonant process, the relevant 4*p* excitation creates the intermediate states $\underline{c}4d^1$ and $\underline{c}4d^2\underline{L}$ which decay resonantly to the $4d^0\underline{L}$ and $4d^1\underline{L}^2$ states. The processes are summarized as follows:

$$4d^0 + h\nu \rightarrow \underline{c}\,4d^1 \rightarrow 4d^0\underline{L} + e, \quad (1)$$

$$\rightarrow 4d^1\underline{L}^2 + e, \quad (2)$$

$$4d^1\underline{L} + h\nu \rightarrow \underline{c}\,4d^2\underline{L} \rightarrow 4d^0\underline{L} + e, \quad (3)$$

$$\rightarrow 4d^1\underline{L}^2 + e, \quad (4)$$

where $\underline{c}$ denotes the 4*p* core hole state. In process (1), the $4d^0\underline{L}$ final state is produced from the $\underline{c}d^1$ state only with a low probability, since the probability involved the Auger integral representing an interionic Coulomb coupling between a metal ion and an adjacent anion. Resonance process (1) can be created interference with direct photoemission process (a). In process (3), the $4d^0\underline{L}$ state is created from the $\underline{c}\,4d^2\underline{L}$ state with a high probability, since the pertinent Auger matrix element is large. This process interferes with the direct emission process (b). The $4d^1\underline{L}^2$ state is also attainable through resonance process (4), but with a probability as low as that in process (1). This resonance process interferes with direct process (c).

Process (2) occurs with a very low probability, since it involves complete interionic Auger transition. The probability integrals include the overlap of the valence hole orbital on the anion with the core hole orbital on the metal ion. Obviously, the direct overlap is very small. Furthermore, there is no pertinent direct process, which can interfere with this process.

From the above findings, two possible final states form by the mixtures of the $4d^0\underline{L}$ and $4d^1\underline{L}^2$ states. The $4d^0\underline{L}$-rich state appears to be responsible for the main valence band, whereas the $4d^1\underline{L}^2$-rich state for the satellite. This assignment and the arguments described above explain why the resonant enhancement of signal S is much less than those of the main bands. Thus, we can conclude that signal S is the charge-transfer satellite structure with $4d^1\underline{L}^2$ in the final state.

4. Conclusions

We have studied the electronic structure of ZrF_4 using RPES. The satellite structure is found with an energy separation of about 12.6 eV below the bonding peak of the valence band. The valence band and the satellite are enhanced at the Zr 4*p* absorption edge. These findings indicate that the $4d^0$ states strongly mixed with the $4d^1\underline{L}$ configuration structure in the ground state.

Acknowledgements

This work was partly supported by the Foundation for Material Science and Technology of Japan (MST Foundation) and the Grant-in-Aid for Science Research (No. 13740191) from the Ministry of Education, Culture, Sports, Science and Technology.

1) P. M. Woodward and T. Vogt: J. Solid State Chem. **138** (1998) 207.
2) M. Ohashi, H. Nakano, S. Yamanaka and M. Hattori: Solid State Ionics **32/33** (1989) 97.
3) Y. Maeno, H. Hashimoto, K. Yoshida, S. Nishizaki, T. Fujita, J. G. Bednorz and F. Lichtenberg: Nature **372** (1995) 532.
4) C. Morant, A. Fernandez, A. R. Gonzalez-Elipe, L. Soriano, A. Stampfl, A. M. Bradshaw and I. M. Sanz: Phys. Rev. B **52** (1995) 11711.
5) H. J. F. Jansen: Phys. Rev. B **43** (1991) 7267.
6) R. Orlando, C. Pisani, C. Roetti and E. Stefanovich: Phys. Rev. B **45** (1992) 592.
7) T. Yokoya, A. Chainani, T. Takahashi, H. Katayama-Yoshida, M. Kasai, Y. Tokura, N. Shanthi and D. D. Sarma: Phys. Rev. B **53** (1996) 8151.
8) J. Zaanen, G. A. Sawatzky and J. W. Allen: Phys. Rev. Lett. **55** (1985) 418.
9) T. Uozumi, K. Okada and A. Kotani: J. Phys. Soc. Jpn. **62** (1993)

2595.
10) K. Okada and A. Kotani: J. Spectrosc. Relat. Phenom. **62** (1993) 131.
11) J. C. Parelebas: J. Phys. **2** (1992) 1392.
12) Z. Zhang, S. Jeng and V. E. Henrich: Phys. Rev. B **43** (1991) 12004.
13) S. Shin, Y. Tezuka, T. Ishii and Y. Ueda: Solid State Commun. **87** (1995) 1051.
14) M. Umeda, Y. Tezuka, S. Shin and A. Yagishita: Phys. Rev. B **53** (1996) 1783.
15) Y. Tezuka, S. Shin, T. Ishii, T. Ejima, S. Suzuki and S. Sato: J. Phys. Soc. Jpn. **63** (1994) 347.
16) T. Higuchi, T. Tsukamoto, N. Sata, M. Ishigame, Y. Tezuka and S. Shin: Phys. Rev. B **57** (1998) 6978.
17) S. Shin, S. Suga, M. Taniguchi, H. Kanzaki, S. Shibuya and T. Yamaguchi: J. Phys. Soc. Jpn. **51** (1982) 906.